Infinite Torsional Motion Generation of a Spherical Parallel Manipulator with Coaxial Input Axes

Iliyas Tursynbek and Almas Shintemirov

***Abstract*— One of the distinct features of 3-RRR spherical parallel manipulators with coaxial input axes (coaxial SPM) is the ability to perform infinite torsional motion of the manipulator mobile platform around its normal vectors. This paper presents a novel approach for infinite torsional motion generation of the coaxial SPM based on the author's revised approach for obtaining unique solutions to SPM kinematics and the methodology for numerical computation of the SPM configuration workspace. Numerical results demonstrate the application of the proposed approach for computing infinite torsional motion of a 3D model of a novel coaxial SPM design.**

I. INTRODUCTION

Spherical parallel manipulators (SPMs) are used in the design of various mechanisms having three rotational degrees of freedom (DOFs), including orientation platforms, haptic devices, rehabilitation and exoskeleton systems, etc. [1]–[5]. In addition, robotic wrists based on SPM architecture may serve as an alternative to the conventional industrial wrist based on serial kinematic architecture [6].

Among numerous types of different 3-DOF SPM topologies that can be synthesized [7]–[11], the 3-RRR type SPMs are one of the first thoroughly analyzed topologies [12]–[14]. Some applications, such as active ball joints, machining tools, or special purpose orientation platforms, require complete $360°$ or infinite torsional motion as one of the design criteria. Such mechanisms can be realized based on the special case of the general 3-RRR type SPM with coaxial input axes (hereafter - coaxial SPM).

The traditional kinematic structure of the coaxial SPM, illustrated in Fig. 1a, was firstly presented in [15] and further analyzed in [16]. This SPM structure was realized in practice in the design of a marine propulsor [17] and a 4-DOF robotic link mechanism [18]. Another structural design of the coaxial SPM was proposed in [19]. This design uses three SPM leg actuators sliding on a circular guide, thus, ensuring a complete torsional motion property of the manipulator. However, to the authors' knowledge, there were no publicly reported research works, outlining theoretical foundations for infinite torsional motion generation of the coaxial SPM, required for its practical applications.

This paper presents a novel approach for infinite torsional motion generation of a 3-RRR SPM with coaxial input axes. The work is built upon the authors' preliminary study [20], reporting the extension to the case of a coaxial SPM of the previously developed approach for computing unique forward and inverse kinematics solutions of a general 3-DOF 3-RRR SPM [21], which was also utilized in the development of offline motion planning and real-time orientation control frameworks for general SPMs in [22], [23].

The paper is organized as follows. Section II gives an overview of the coaxial SPM kinematics, whereas the generation of infinite torsional motions is presented in Section III. Subsequently, Section IV outlines the effects of singularities and link collisions on the coaxial SPM configuration space considering the infinite torsional motion of the manipulator. Section V presents the numerical results of the infinite torsional motion generation of the coaxial SPM simulation model. Finally, conclusions are drawn in Section VI.

II. KINEMATICS OF THE COAXIAL SPM

This section introduces the notation and terminology to be used throughout the paper, as well as presents the revised approach for obtaining unique solutions to the inverse kinematics problem, initially proposed by the authors in [20].

A. Kinematic Model

The coaxial SPM consists of the *mobile platform*, which undergoes a 3-DOF spherical motion, and is connected to a stationary *base* via three equally-spaced legs numbered as $i = 1, 2, 3$ in the counter-clockwise direction. Each leg is composed of two curved *links*: *proximal* (lower) and *distal* (upper). The angles α_1 and α_2 define curvatures of these links, respectively. The geometry of the mobile platform is defined by the angle β. The base joints, i.e. *input joints*, have coaxial alignment as shown in Fig. 1a, allowing infinite torsional motion of the SPM mobile platform. The axes of the base, the intermediate, and the mobile platform joints intersect at the *center of rotation*, and are defined by the unit vectors $\mathbf{u}_i$, $\mathbf{w}_i$, and $\mathbf{v}_i$, for $i = 1, 2, 3$, respectively, directed from the center of rotation towards corresponding joints.

The stationary right-handed orthogonal coordinate system with its origin located at the center of rotation is shown in Fig. 1a. The *z*-axis is normal to the base and is directed upwards, while the *x*-axis is located in the plane formed by the *z*-axis and the unit vector $\mathbf{w}_1$ at the home configuration. The *y*-axis is determined by the right-hand rule. The *home configuration* of the coaxial SPM is chosen such that all three proximal links are located $120°$ apart. In this case, the mobile platform is horizontal and its normal vector coincides with the positive *z*-axis.

Input joint positions, constituting vector $\boldsymbol{\theta} \triangleq \left[\theta_1, \theta_2, \theta_3\right]^T$, are measured from the planes defined by the *z*-axis and unit

All authors are with the School of Engineering and Digital Sciences, Nazarbayev University, 53 Kabanbay batyr Ave., Nur-Sultan (Astana) Z05H0P9, Kazakhstan. iliyas.tursynbek@nu.edu.kz; ashintemirov@nu.edu.kz

Corresponding author: A. Shintemirov

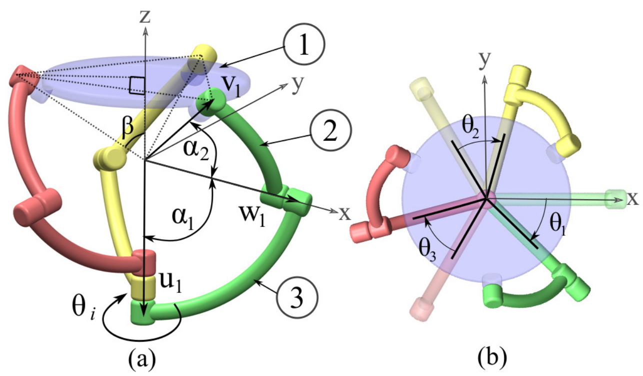

Fig. 1: The coaxial SPM: (a) kinematic model (1 - mobile platform, 2 - distal link, 3 - proximal link), (b) positive direction of input joint positions with respect to the home configuration (shown as transparent footprint).

vectors $\mathbf{w}_i, = 1,2,3$, at the home configuration to the planes of the proximal links of the corresponding legs with the clockwise direction being the positive direction as illustrated in Fig. 1b. At the home configuration, the vector of input joint positions is set to $\boldsymbol{\theta} = \left[0,0,0\right]^T$.

Under the prescribed coordinate system, the unit vectors $\mathbf{u}_i$, $i = 1,2,3$, of the base joints are defined as $\mathbf{u}_i = \left[0,0,-1\right]^T$. The unit vectors $\mathbf{w}_i$, $i = 1,2,3$, of the intermediate joints are expressed as:

$$\mathbf{w}_i = \begin{bmatrix} \cos(\eta_i - \theta_i)\sin\alpha_1 \\ \sin(\eta_i - \theta_i)\sin\alpha_1 \\ -\cos\alpha_1 \end{bmatrix}, \tag{1}$$

where $\eta_i = 2(i-1)\pi/3$, $i = 1,2,3$.

The unit vectors $\mathbf{v}_i$, $i = 1,2,3$, of the mobile platform joints are used to define the orientation of the coaxial SPM.

Note: In this paper, the direction of legs numbering (counter-clockwise), definition of the positive direction of rotation (clockwise, right-hand rule applied on vectors $\mathbf{u}_i$, $i = 1,2,3$), and alignment of the home configuration with the fixed coordinate system are modified from that of [20]. This is done in order to comply with the earlier works of Gosselin *et al.* [12]–[14] and to preserve the notation and definition consistency. These changes resulted in a slight modification of the expression of the unit vectors $\mathbf{w}_i$, $i = 1,2,3$, as shown in (1) and the coefficients A_i, B_i, and C_i used for obtaining unique inverse kinematic solutions discussed in the next subsection.

B. Inverse Kinematics

The inverse kinematics problem is defined by computing the vector of input joint positions $\boldsymbol{\theta}$ corresponding to a given orientation of the mobile platform described by the unit vectors $\mathbf{v}_i$, $i = 1,2,3$.

The geometric relation between the intermediate and the mobile platform's joints is described as:

$$\mathbf{w}_i \cdot \mathbf{v}_i = \cos\alpha_2, \quad i = 1,2,3, \tag{2}$$

After substituting (1) in (2) and performing the derivation process, the details of which are omitted here due to space limitations, the following three uncoupled equations for each input joint position θ_i, $i = 1,2,3$ are obtained [13]:

$$A_i T_i^2 + 2 B_i T_i + C_i = 0, \quad i = 1,2,3, \tag{3}$$

with

$$T_i = \tan\left(\frac{\theta_i}{2}\right). \tag{4}$$

Coefficients A_i, B_i, and C_i are formulated as follows:

$$\begin{aligned} A_i &= -\cos\eta_i \sin\alpha_1 v_{ix} - \sin\eta_i \sin\alpha_1 v_{iy} \\ &\quad -\cos\alpha_1 v_{iz} - \cos\alpha_2; \\ B_i &= \sin\eta_i \sin\alpha_1 v_{ix} - \cos\eta_i \sin\alpha_1 v_{iy}; \\ C_i &= \cos\eta_i \sin\alpha_1 v_{ix} + \sin\eta_i \sin\alpha_1 v_{iy} \\ &\quad -\cos\alpha_1 v_{iz} - \cos\alpha_2, \end{aligned} \tag{5}$$

where v_{ix}, v_{iy}, and v_{iz} are the components of the unit vectors $\mathbf{v}_i$, $i = 1,2,3$.

The equations (3) are decoupled quadratic equations with two roots for each T_i, resulting in eight total combinations of possible input joint positions, referred to as the *working modes*. By selecting the combination corresponding to the roots with added square root of the discriminant (the definition of the positive direction of rotation), the coaxial SPM will be operating in the *l-l-l* working mode as discussed in [20], [23].

The computation procedure of the unique solutions for the coaxial SPM inverse kinematics problem is outlined in the revised Algorithm 1, that was initially formulated and experimentally verified by the authors in [20].

Algorithm 1: Obtaining unique solution to the coaxial SPM inverse kinematics

Input: $\mathbf{v}_i$, $i = 1,2,3$, α_1, α_2, η_i
Output: Vector of input joint positions $\boldsymbol{\theta}$

for $i \leftarrow 1$ **to** 3 **do**
  Calculate A_i, B_i, C_i using (5) given $\mathbf{v}_i$, α_1, and α_2;
  Solve equation (3) for T_i;
  Find θ_i using (4) and by selecting the solution corresponding to the root with added square root of the discriminant (for *l-l-l* working mode);
return θ_i, $i = 1,2,3$.

III. Infinite Torsional Motion Generation

One of the distinct features of the coaxial SPM, compared to other special kinematic architectures of the 3-RRR SPMs (e.g., manipulator with coplanar actuators [13] and the *Agile Eye* [24]), is the ability to perform infinite torsional motion of the mobile platform around its normal vector as shown in Fig. 2. In order to perform such motion, a sequence of input joint positions ($\boldsymbol{\theta}$'s), i.e. actuator motion trajectories, needs to be generated. This section addresses the process

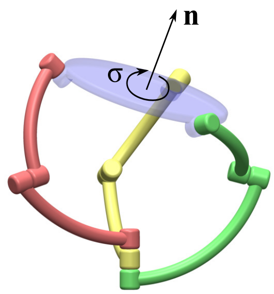

Fig. 2: Rotation of the mobile platform around its normal vector $\mathbf{n}$ by an angle σ.

of generating motion trajectories for the infinite torsional motion.

The orientation of the coaxial SPM is described by the unit vectors $\mathbf{v}_i$, $i = 1, 2, 3$. Using this description, the rotation of the mobile platform around its normal vector $\mathbf{n}$ is formulated as the rotation of the unit vectors $\mathbf{v}_i$, $i = 1, 2, 3$, around the same vector $\mathbf{n}$, which is defined as:

$$\mathbf{n} = \frac{\mathbf{v}_1 + \mathbf{v}_2 + \mathbf{v}_3}{\|\mathbf{v}_1 + \mathbf{v}_2 + \mathbf{v}_3\|}. \tag{6}$$

The instantaneous orientation of the mobile platform during the torsional motion is defined by the unit vectors $\mathbf{v}_{i,rot}$, $i = 1, 2, 3$, and is calculated using the Rodrigues' rotation formula [25]:

$$\begin{aligned} \mathbf{v}_{i,rot} = & \, \mathbf{v}_i \cos\sigma + (\mathbf{v}_i \times \mathbf{n}) \sin\sigma \\ & + \mathbf{n}(\mathbf{n} \cdot \mathbf{v}_i)(1 - \cos\sigma), \quad i = 1, 2, 3, \end{aligned} \tag{7}$$

where σ is an angle of the platform's rotation measured from the starting configuration to the resultant rotational instance as illustrated in Fig. 2.

To generate motion trajectories for the infinite torsional motion, a single $360°$ torsional rotation of the mobile platform is sampled into a sequence of instances, and at each instance the procedure for obtaining unique inverse kinematics solution (Algorithm 1) is implemented. As the result, the sequence of input joint positions $\boldsymbol{\theta}_{rot}$ leading to the SPM torsional motion around the vector $\mathbf{n}$ is generated. The infinite torsional motion of the coaxial SPM is achieved by applying the obtained sequence $\boldsymbol{\theta}_{rot}$ over and over again. However, each subsequent rotation has to be adjusted by the addition of an extra $360°$ (2π) to the sequence $\boldsymbol{\theta}_{rot}$ once the current rotation is completed. This condition is imposed by Algorithm 1 that returns output values on the scale from $-180°$ $(-\pi)$ to $+180°$ $(+\pi)$ due to the nature of arc-tangent in (4). Therefore, each time the mobile platform passes through the same orientation during the infinite torsional motion it is treated in the same way by Algorithm 1 and continuity of the input sequence is violated.

Another important issue to consider is a *link surpass*. It is a situation that happens when proximal links have to pass through each other to reach specific orientation. For example, the input position $\boldsymbol{\theta} = \left[160°, 160°, 190°\right]^T$ is obtained from Algorithm 1 as $\boldsymbol{\theta} = \left[160°, 160°, -170°\right]^T$, which, if applied to the actuators, will force the *proximal link 3* to rotate in the opposite direction with respect to the remaining proximal links, thus, resulting in a link collision. Realizable in some computer simulations but not with the physical prototype this type of input positions has to be accounted and adjusted by the addition of an extra $360°$ (2π) to the link with the negative input position, ensuring only a positive direction of rotation.

IV. Configuration Space of the Coaxial SPM

This section describes the numerical method used for computing the space of feasible configurations of the coaxial SPM, taking the infinite torsional motion of the manipulator into account.

A. Singularity Detection

During the motion of the manipulator, it is desirable to avoid singular and near-singular configurations as they degenerate its controllability. For this purpose, a conditioning index $\zeta(\mathbf{J}) \in (0, 1)$ is widely used as an indicator, where $\mathbf{J}$ denotes a Jacobian matrix of the SPM. A value of $\zeta(\mathbf{J})$ close to 0 corresponds to a near-singular configuration, while $\zeta(\mathbf{J})$ equal to 1 coincides with a non-singular configuration. A threshold value $\zeta(\mathbf{J})_{min}$ can be used to differentiate between near-singular and non-singular configurations.

The reader is referred to [22] for the concise description of the singularity analysis of the general SPM, which includes the derivation of $\zeta(\mathbf{J})$. In [20] the authors described the approach for obtaining unique forward kinematics solution required in [22] to obtain the unit vectors $\mathbf{w}_i$ and $\mathbf{v}_i$, $i = 1, 2, 3$, given a vector of input joint positions $\boldsymbol{\theta}$.

For a sampled rotational motion of the mobile platform around its normal vector, the conditioning index $\zeta(\mathbf{J})$ is calculated at each instance. If any of $\zeta(\mathbf{J})$ values during the rotation is below $\zeta(\mathbf{J})_{min}$, this rotational motion is treated as not singularity-free and, therefore, is neglected.

B. Link Collision Detection

Some configurations of the coaxial SPM lead to link collisions. In order to detect such configurations, a widely utilized by robotics community free access robot simulator software CoppeliaSim (former V-REP) [26] is used as detailed in [27]. It allows physical simulation of parallel manipulators and their motion control through a remote API client from external environments such as MATLAB and ROS. The simulator has a built-in collision detection module that signals the remote client about a link collision occurrence during a simulated manipulator motion. During the simulation, the collision state of each registered collision object can then be visualized with a different coloring. Collision check routing is repeated for each rotational instance. If any of the manipulator's link collide during the torsional motion, this motion is treated as not safe and, thus, is neglected.

C. Space of Feasible Configurations

Combining the procedures outlined in the previous subsections, it is possible to numerically determine if a given configuration $\boldsymbol{\theta}$ of the coaxial SPM is feasible or not. Unfeasible configurations are the ones that lead to a singularity or near-singularity, or the ones that cause link collisions. A space of feasible configurations for the coaxial SPM is generated by iterating through a 3D grid of all possible configurations and verifying whether they are feasible or not. A uniform sampling is employed for the simplicity, i.e. $\delta \triangleq \theta_{i,j+1} - \theta_{i,j}$ is constant.

For the reduction of the amount of computations, it is reasonable to exclude configurations which lead to the link surpass (Section III), as no real-world manipulator is able to perform such motions. Link surpass happens when an actuated joint position is greater than that of the next joint in the positive (clockwise) direction of movement, i.e. $\theta_3 - \theta_2$, $\theta_2 - \theta_1$, or $\theta_1 - \theta_3$ should not be greater than $120°$ (the thickness of links is ignored). The remaining set is then analyzed for feasibility. As the result of this procedure, a set $\mathcal{V}$ is created. It represents the union of all nodes corresponding to feasible configurations of the coaxial SPM.

V. Results and Discussion

Numerical verification of the proposed approach for infinite torsional motion generation is conducted using a example model of the coaxial SPM with the following geometrical parameters: $\alpha_1 = 45°$, $\alpha_2 = 90°$, and $\beta = 90°$. The model was designed in Solidworks 3D CAD software (`www.solidworks.com`) and is presented in rendered form in Fig. 3a. A simplified version of the model was imported to CoppeliaSim (V-REP) robot simulator (Fig. 3b), where it was used for the link collision detection procedures [27]. MATLAB (`www.mathworks.com`) was used as the remote API client for the SPM motion control and collision data recording, as well as singularity detection calculations.

A. Computation of the Space of Feasible Configurations

The space of feasible configurations was computed by verifying whether a given vector of input joint positions $\boldsymbol{\theta}$ would result in a singular or near-singular configuration or lead to a link collision of the manipulator. A set of uniformly-sampled input configurations $\boldsymbol{\theta}$ between $0°$ and $360°$, with spacing $\delta = 5°$ was used for the numerical computation of the space (a total of 373,248 test nodes). Initially the set of SPM configurations shown in Fig. 4a was obtained after excluding configurations that resulted in link surpass. All nodes in this test set were then passed through the singularity detection procedure with the threshold value of the conditioning index $\zeta(\mathbf{J})_{min} = 0.2$. As a result, the remaining nodes were separated into several subsets, belonging to the different assembly modes of the manipulator as shown in Fig. 4b (cross-sectional view in the middle of the diagonal axis). The configurations that passed the singularity check then were tested for link collisions and the final set of feasible configurations $\mathcal{V}$ of the coaxial SPM model was obtained as shown in Fig. 4c.

The obtained set $\mathcal{V}$ spans diagonally from $\boldsymbol{\theta} = \left[0°, 0°, 0°\right]^T$ to $\boldsymbol{\theta} = \left[360°, 360°, 360°\right]^T$ with the deviation of each joint input angle not greater than $100°$. This result dictates that given the two fixed actuators with the same

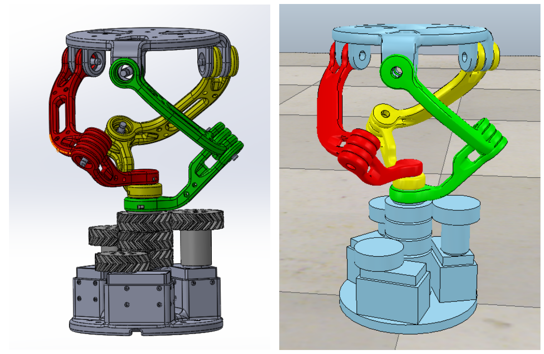

(a) (b)

Fig. 3: A 3D CAD model (a) and a simulation model (b) of the coaxial SPM.

input positions, the third one cannot exceed $\pm 100°$ from that value; otherwise the manipulator links will collide. This value is specific for the given coaxial SPM model. Moreover, the obtained set $\mathcal{V}$ is not limited by $0°$ and $360°$ on the main diagonal, but extends infinitely in positive and negative directions. This result confirms that the manipulator under study is capable of the infinite torsional motion.

B. Infinite Torsional Motion Generation

Consider the case of infinite torsional motion generation of the coaxial SPM mobile platform with the orientation described as:

$$\begin{aligned} \mathbf{v}_1 &= \left[-0.8905,\ 0.1896,\ -0.4136\right]^T; \\ \mathbf{v}_2 &= \left[0.4129,\ -0.9058,\ -0.0953\right]^T; \\ \mathbf{v}_3 &= \left[0.4722,\ 0.7160,\ 0.5096\right]^T. \end{aligned} \tag{8}$$

Rotational instances of these unit vectors $\mathbf{v}_{i,rot}$, $i = 1, 2, 3$, are calculated by applying (7). The sequence of input joint positions is then generated by applying Algorithm 1 at each rotational instance. Imposing the computed input joint positions to the coaxial SPM model in CoppeliaSim robot simulator, following the procedure outlined in Section III, results in the infinite torsional rotation of the manipulator as shown in Fig. 5 for six subsequent input joint position instances. The video demonstration of the simulated infinite torsional motion of the coaxial SPM model is available at the author's research lab web-site `www.alaris.kz`.

Figure 6 presents time evolutions of the three input joint rates of change applied to the coaxial SPM model for realizing its torsional motion in Fig.5. It is seen that all the input joint rates of change are periodic and identical with $120°$ phase shifts between each other. This implies that only one input joint trajectory can be generated; the remaining input trajectories are obtained by adding $120°$ and $240°$ phase shifts.

Figure 7 demonstrates the generated helix-shaped manipulator input joint trajectory lying inside the space of joint feasible configurations of the coaxial SPM model, expanded in both directions of rotation, thus confirming that the complete

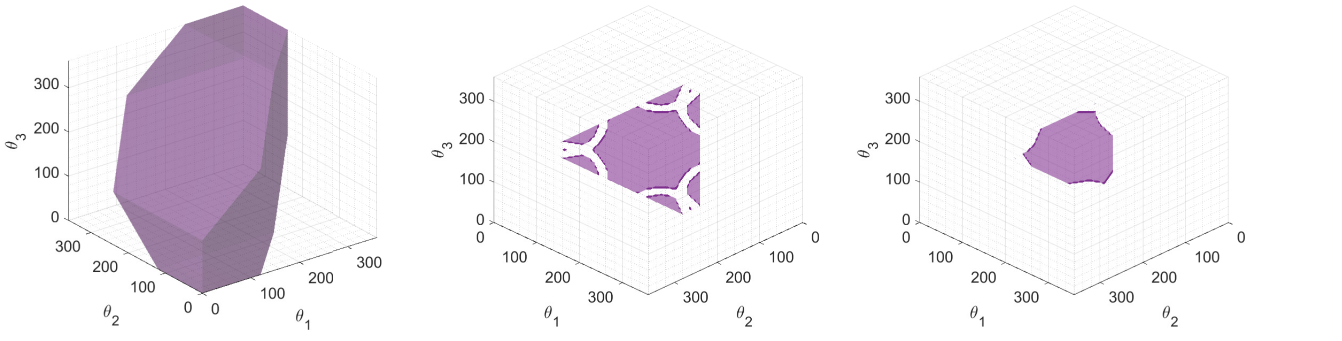

(a) (b) (c)

Fig. 4: Estimation process of the space of feasible configurations: (a) set of nodes with no link surpass, (b) set of singularity free nodes (cross-section view), (c) set of singularity and link collisions free nodes (cross-section view).

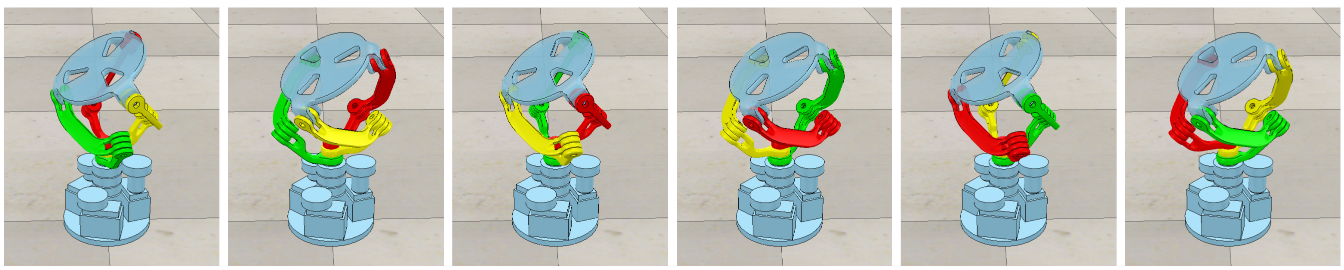

(a) $\sigma = 0^{\circ}$ (b) $\sigma = 60^{\circ}$ (c) $\sigma = 120^{\circ}$ (d) $\sigma = 180^{\circ}$ (e) $\sigma = 240^{\circ}$ (f) $\sigma = 300^{\circ}$

Fig. 5: The coaxial SPM rotational instances about normal vector **n**.

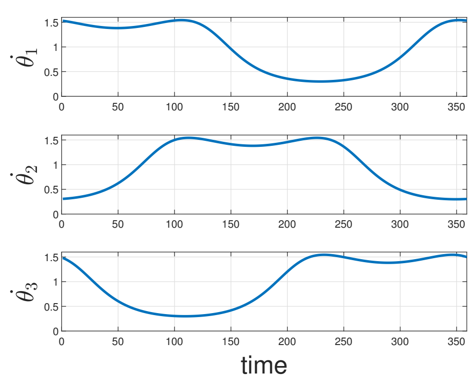

Fig. 6: Input joint rates of change of the coaxial SPM model.

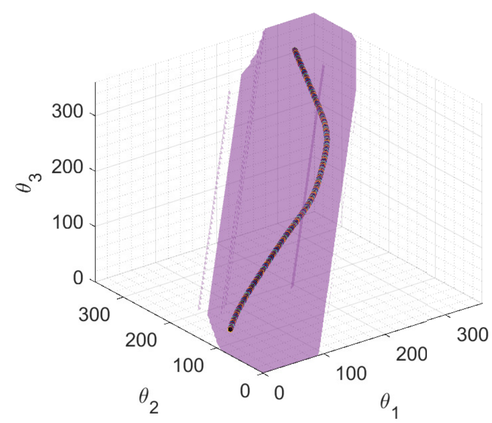

Fig. 7: Example of the torsional motion joint trajectory of the coaxial SPM model.

360° torsional rotation is realizable in this example case. However, in certain other orientations of the coaxial SPM model, the part of the input joint motion trajectory could exceed the computed feasible joint workspace, indicating that the infinite torsional motion is not possible at those orientations.

VI. Conclusions

This paper presented a novel approach for infinite torsional motion generation of a 3-RRR SPM with coaxial input shafts. A revised approach for obtaining unique inverse kinematics solutions was presented. It was used for generating input joint trajectories of the coaxial SPM, that is able to realize infinite torsional motion within the precomputed space of feasible configurations. The presented results of the numerical case study using the coaxial SPM simulation model verified viability of the proposed approach and revealed periodic nature and similarities between the input joint velocities. The reported theoretical and numerical results will be further analyzed and utilized in real-time orientation control system design for a physical prototype of the coaxial SPM.

References

[1] C. Gosselin, E. S. Pierre, and M. Gagne, "On the development of the Agile Eye," *IEEE Robotics & Automation Magazine*, vol. 3, no. 4, pp. 29–37, 1996.

[2] L. Birglen, C. Gosselin, N. Pouliot, B. Monsarrat, and T. Laliberte, "SHaDe, a new 3-DOF haptic device," *IEEE Transactions on Robotics and Automation*, vol. 18, no. 2, pp. 166–175, 2002.

[3] M. Malosio, S. P. Negri, N. Pedrocchi, F. Vicentini, M. Caimmi, and L. M. Tosatti, "A spherical parallel three degrees-of-freedom robot for ankle-foot neuro-rehabilitation," in *Proceedings of the Annual International Conference of the IEEE EMBS*, 2012, pp. 3356–3359.

[4] Y. Du, R. Li, D. Li, and S. Bai, "An ankle rehabilitation robot based on 3-RRS spherical parallel mechanism," *Advances in Mechanical Engineering*, vol. 9, no. 8, pp. 1–8, 2017.

[5] S. Sadeqi, S. P. Bourgeois, E. J. Park, and S. Arzanpour, "Design and performance analysis of a 3-RRR spherical parallel manipulator for hip exoskeleton applications," *Journal of Rehabilitation and Assistive Technologies Engineering*, vol. 4, 2017.

[6] N. M. Bajaj, A. J. Spiers, and A. M. Dollar, "State of the art in artificial wrists: A review of prosthetic and robotic wrist design," *IEEE Transactions on Robotics*, vol. 35, no. 1, pp. 261–277, 2019.

[7] Y. Fang and L.-W. Tsai, "Structure synthesis of a class of 3-DOF rotational parallel manipulators," *IEEE Transactions on Robotics and Automation*, vol. 20, no. 1, pp. 117–121, 2004.

[8] X. Kong and C. M. Gosselin, "Type synthesis of 3-DOF spherical parallel manipulators based on screw theory," *Journal of Mechanical Design*, vol. 126, no. 1, pp. 101–108, 2004.

[9] X. Kong and C. Gosselin, "Type synthesis of three-degree-of-freedom spherical parallel manipulators," *The International Journal of Robotics Research*, vol. 23, no. 3, pp. 237–245, 2004.

[10] M. Karouia and J. M. Hervé, "Non-overconstrained 3-DOF spherical parallel manipulators of type: 3-RCC, 3-CCR, 3-CRC," *Robotica*, vol. 24, no. 01, p. 85, 2005.

[11] Y. Qi, T. Sun, Y. Song, and Y. Jin, "Topology synthesis of three-legged spherical parallel manipulators employing lie group theory," *Proceedings of the Institution of Mechanical Engineers, Part C: Journal of Mechanical Engineering Science*, vol. 229, no. 10, pp. 1873–1886, 2014.

[12] C. Gosselin and J. Angeles, "The optimum kinematic design of a spherical three-degree-of-freedom parallel manipulator," *Journal of Mechanisms, Transmissions, and Automation in Design*, vol. 111, no. 2, pp. 202–207, 1989.

[13] C. Gosselin and E. Lavoie, "On the kinematic design of spherical three-degree-of-freedom parallel manipulators," *The International Journal of Robotics Research*, vol. 12, no. 4, pp. 394–402, 1993.

[14] C. M. Gosselin, J. Sefrioui, and M. J. Richard, "On the direct kinematics of spherical three-degree-of-freedom parallel manipulators of general architecture," *Journal of Mechanical Design*, vol. 116, no. 2, pp. 594–598, 1994.

[15] H. Asada and J. Granito, "Kinematic and static characterization of wrist joints and their optimal design," in *Proceedings of the 1985 IEEE International Conference on Robotics and Automation (ICRA 1985)*, vol. 2, Mar. 1985, pp. 244–250.

[16] C. Gosselin, J. Sefrioui, and M. Richard, "On the direct kinematics of spherical three-degree-of-freedom parallel manipulators with a coplanar platform," *Journal of Mechanical Design*, vol. 116, no. 2, pp. 587–593, 1994.

[17] B. Sudki, M. Lauria, and F. Noca, "Robotic penguin-like propulsor with novel spherical joint," in *Proceedings of the Third International Symposium on Marine Propulsors*, 2013.

[18] J. Lee, J. Noh, S. Lee, and W. Yang, "A novel 4-DoF robotic link mechanism with e-CoSMo: Kinematics based torque analysis," in *2019 IEEE/RSJ International Conference on Intelligent Robots and Systems (IROS)*, 2019.

[19] S. Bai and M. R. Hansen, "Evaluation of workspace of a spherical robotic wrist," in *2007 IEEE/ASME International Conference on Advanced Intelligent Mechatronics (AIM 2007)*, 2007.

[20] I. Tursynbek, A. Niyetkaliyev, and A. Shintemirov, "Computation of unique kinematic solutions of a spherical parallel manipulator with coaxial input shafts," in *2019 IEEE 15th International Conference on Automation Science and Engineering (CASE)*, 2019.

[21] A. Niyetkaliyev and A. Shintemirov, "An approach for obtaining unique kinematic solutions of a spherical parallel manipulator," in *Proceedings of the 2014 IEEE/ASME International Conference on Advanced Intelligent Mechatronics (AIM 2014)*, 2014, pp. 1355–1360.

[22] A. Shintemirov, A. Niyetkaliyev, and M. Rubagotti, "Numerical optimal control of a spherical parallel manipulator based on unique kinematic solutions," *IEEE/ASME Transactions on Mechatronics*, vol. 21, no. 1, pp. 98–109, 2016.

[23] T. Taunyazov, M. Rubagotti, and A. Shintemirov, "Constrained orientation control of a spherical parallel manipulator via online convex optimization," *IEEE/ASME Transactions on Mechatronics*, vol. 23, no. 1, pp. 252–261, 2018.

[24] C. M. Gosselin and J.-F. Hamel, "The agile eye: a high-performance three-degree-of-freedom camera-orienting device," in *Proceedings of the 1994 IEEE International Conference on Robotics and Automation (ICRA 1994)*, 1994, pp. 781–786.

[25] B. Siciliano and O. Khatib, *Springer Handbook of Robotics*. Berlin, Heidelberg: Springer-Verlag, 2007.

[26] M. F. E. Rohmer, S. P. N. Singh, "Coppeliasim (formerly V-REP): a versatile and scalable robot simulation framework," in *Proc. of The International Conference on Intelligent Robots and Systems (IROS)*, 2013, www.coppeliarobotics.com.

[27] I. Tursynbek and A. Shintemirov, "Modeling and simulation of spherical parallel manipulators in CoppeliaSim (V-REP) robot simulator software," in *International Conference "Nonlinearity, Information and Robotics"*, 2020.